DOI: https://doi.org/10.14525/JJCE.v20i1.04



Jordan Journal of Civil Engineering

Journal homepage: https://jjce.just.edu.jo



GIS-driven Analysis of Seasonal Variations in Air Quality in Urban Areas: Case Study of Navi Mumbai, India

Sujaya Wadekar 1)*, S. Sangita Mishra 1)

¹⁾ Amity School of Engineering and Technology, Amity University Maharashtra, Mumbai 410206, India. * Corresponding Author. E-Mail: sujayacecila@yahoo.co.in

ARTICLE INFO

Article History: Received: 9/2/2025 Accepted: 19/8/2025

ABSTRACT

The rapid growth of road transportation is significantly degrading air quality, with pollutants, like PM_{10} , SO_2 , and NO_x , contributing to respiratory issues and serious health risks. This study analyzes the spatial distribution and seasonal variation of PM_{10} , NO_x , and SO_2 using daily data from 23 monitoring stations across Navi Mumbai and Thane from 2014 to 2023.

Focusing on monsoon, pre-monsoon, post-monsoon, and winter seasons, the study integrates GIS-based spatial interpolation techniques-to-explore how seasonal changes influence pollutant levels. Results reveal persistently high PM_{10} concentrations across all stations. Despite the monsoon season's cleansing effect, moderate-to-poor air quality persisted due to continuous vehicular and industrial emissions. Notably, Kharghar, Taloja, and Kalamboli recorded PM_{10} levels of 257 $\mu g/m^3$ and 217 $\mu g/m^3$ in 2014-2015. Nerul peaked at 600 $\mu g/m^3$ in the 2017 pre-monsoon season, surging to 1000 $\mu g/m^3$ on June 21, 2023. Post-monsoon readings in 2014 showed Airoli at 320.99 $\mu g/m^3$ and Glaxo premises at 496 $\mu g/m^3$.

Persistent pollution in areas, like Pimpaleshwar Mandir and Ulwe, highlights the need for continuous monitoring. Since 2020, NO levels have worsened, particularly in industrial zones, such as Mahape and Nerul, shifting from moderate to very poor across seasons. Figures 7, 9, and 11 illustrate these trends. In contrast, SO_2 concentrations remained stable, with slight post-2020 increases in Mahape and Pimpaleshwar Mandir during post-monsoon periods.

GIS analysis helped identify pollution hotspots and assess regulatory effectiveness. This study highlights the critical need for ongoing air quality monitoring and targeted mitigation strategies to address escalating public health concerns in the region.

Keywords: PM₁₀, NO_x, SO₂ GIS, Spatial interpolation, Air quality mapping.

INTRODUCTION

Industrial and economic activities, such as waste management, thermal power plants, and vehicular traffic, significantly affect tropospheric air quality. These activities alter the composition of the surrounding air, impacting the atmosphere at global, regional, and local levels (Kuldeep et al., 2022). The rapid

urbanization of cities, like Delhi and Mumbai in 21st-century India, is largely attributed to rural-to-urban migration (Patel & Burkle, 2012). Urbanization and population growth adversely influence water, air, and soil quality (Huff & Angeles, 2011).

Air pollution has emerged as one of the most pressing global challenges. It involves the presence of airborne substances, with pollutant concentrations exceeding normal levels due to a mix of natural and anthropogenic activities (Pathakoti et al., 2021). These substances have been shown to cause detrimental effects on human and animal health, damage vegetation, degrade materials, and harm the environment (Othman et al., 2010). Urban air pollution in Indian cities is marked by elevated levels of pollutants, such as carbon monoxide (CO), sulfur dioxide (SO₂), particulate matter (PM), and nitrogen oxides (NO_x), which primarily originate from the automotive industry. For instance, vehicles running on diesel and petrol emit pollutants, like SO₂, NO_x, hydrocarbons (HCs), volatile organic compounds (VOCs), PM, and CO, significantly contributing to urban air quality degradation (Bosco et al., 2005, Batterman et al., 2007, Wu et al., 2011, Emami et al., 2018, Marc et al., 2016). The statistical correlation between PM₁₀, SO₂, and NO_x plays a vital role in understanding air pollution dynamics and improving air quality assessments. These pollutants often share common sources, such as vehicular emissions, industrial activities, and combustion of fossil fuels, which is reflected in their correlated concentration levels. A strong positive correlation between PM₁₀ and NO_x typically indicates traffic-related emissions, while a moderate correlation between SO₂ and the other pollutants may point to industrial processes or power generation. Analyzing these correlations helps in identifying the dominant sources of pollution within a given area, providing a scientific basis for implementing targeted control measures. Moreover, correlation analysis is essential in predicting pollution episodes, particularly in relation to seasonal variations and meteorological conditions. Understanding how these pollutants vary together also supports the calibration of air quality models, allowing for more accurate simulations and forecasts. From a public health perspective, the combined presence of highly correlated pollutants can lead to compounded respiratory effects, making their joint assessment critical for health risk evaluations. Traffic variables, such as vehicular speed, traffic volume, and road gradient, play a crucial role in influencing vehicle emissions and concentrations of air pollutants (CO, NO, TVOCs, SO₂), underscoring their importance in urban planning for evaluating and modeling environmental impacts, like air and noise pollution; a strong correlation between these traffic parameters and pollutant levels was observed across multiple sampling locations (Zaydoun et al., 2019).

Ultimately, the correlation among PM₁₀, SO₂, and

NO_x not only informs environmental policy and regulatory standards, but also facilitates effective air quality management by highlighting pollution hotspots and the efficiency of mitigation strategies.

Understanding the composition of pollutants, such as PM₁₀, SO₂, and NO_x, requires a systematic approach to identify their potential sources in urban areas to mitigate environmental challenges associated with air quality. Many countries are actively monitoring air quality to enhance policy-making mechanisms (Mendoza et al., 2019). In India, the Central Pollution Control Board (CPCB), headquartered in New Delhi, oversees air quality monitoring through the NAAQMS (National Ambient Air Quality Monitoring Series), which is part of the NAMP (National Air Monitoring Programme). The reviewed literature reveals that despite various technological and methodological advancements, a significant research gap persists in developing an integrated, standardized, and comprehensive framework for air pollution monitoring and forecasting. Ranjeet S. Sokhi et al. (April 2022) highlighted the challenges in mapping pollutants and the need to combine ground station and remote sensing data, while Rongjin Yang et al. (March 2022) emphasized the lack of accurate datasets in China due to cost limitations and introduced an IPv6based system for enhanced monitoring. Vasilis Evagelopoulos et al. (March 2022) presented a cloudbased system, AirDMS, capable of managing large datasets, did not address cross-regional standardization. Suman (Aug. 2020) criticized the variability in air quality indices across Indian cities and argued for a more accurate depreciation index. Xiaoxin Fu et al. (Feb. 2016) explored the link between PM_{2.5}, humidity, and visibility, indicating the complexity of pollutant interactions. Terry Gordon et al. (June 2018) stressed the importance of personal exposure monitoring, especially in the context of Indian rural and urban disparities. Ankur Sati & Manju Mohan (2014) pointed out the dominant role of regional pollution under adverse climatic conditions, and Subrata Chattopadhyay et al. (2010) used GIS to analyze seasonal variations in air quality. However, across all these studies, a common gap remains: the absence of a unified, low-cost, and scalable system that combines indoor-outdoor pollution data, personal exposure, and real-time analytics using remote sensing, ground stations, and GIS tools, along with standardized indices for inter-regional comparison.

Public demand compelled authorities to implement

various control measures, leading to noticeable air quality improvements between 1991 and 2003 (Gupta & Kumar, 2006). During this period, industries contributing to air pollution relocated to peripheral areas, vehicles adopted advanced technologies, and low emission fuels were introduced. However, Mumbai's air quality has since deteriorated, with PM₁₀ and Suspended Particulate Matter (SPM) levels exceeding the CPCB's recommended limits, as reported by the National Environmental Engineering Research Institute (NEERI, 2013). For residential areas, the permissible limits for PM_{10} and SPM are $60 \mu g/m^3$ and 140 µg/m³, respectively. Studies on air pollution in megacities have further identified high concentrations of total suspended particles (TSPs) as a primary concern (Mage et al., 1996). Elevated levels of particulate matter are widely recognized for their significant adverse effects on health and the environment (Chhabra et al., 2010; Kampa & Castanas, 2008; Srivastava & Kumar, 2002; Zhou et al., 2014; Kristiansson et al., 2015).

STUDY AREA

The study area encompasses 337.49 km² in Maharashtra, covering 23 stations across Navi Mumbai and parts of the Thane district. It is situated between longitudes 72.90° to 73.15° East and latitudes 18.90° to 19.30° North. Navi Mumbai, a rapidly urbanizing city, is highly vulnerable to climate risks, such as heatwaves, forest fires, and deteriorating air quality due to urbanization. The 1960s Regional Plan for the Mumbai Metropolitan Region (MMR) designated large industrial zones near Parsik Hills and Taloja, adjacent to Navi Mumbai. These zones host highly polluting industries, resulting in severe health and environmental challenges. In 2019, the Maharashtra Pollution Control Board highlighted a rise in air-borne diseases linked to these industries. Details of the study area, along with air quality monitoring stations, are illustrated in Figure 1.

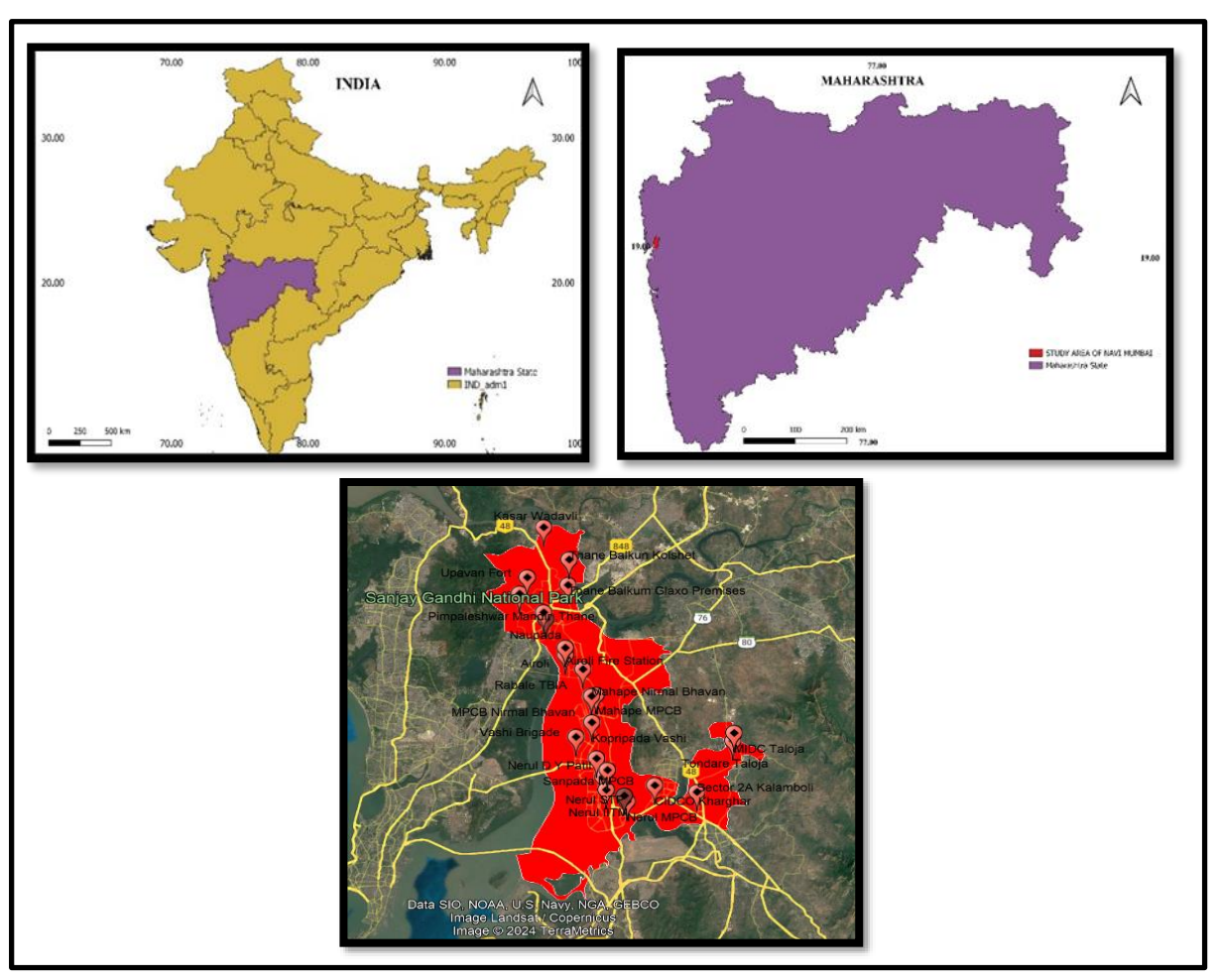


Figure 1. Study area location map and monitoring stations

METHODOLOGY

Collection and Pre-processing of Air Quality Data

The data is collected from various ground stations set

up by Central Pollution Control Board (CPCB) and Maharashtra Pollution Control Board (MPCB). The locations of the monitoring stations are shown in Table 1.

Table 1. Air	quality	monitoring	stations
--------------	---------	------------	----------

Sr. No.	AQM_Stations	Latitude	Longitude	Sr. No.	AQM_Stations	Latitude	Longitude
1	Airoli	19.158	72.98	13	MPCB Nirmal Bhavan	19.114	73.015
2	Nerul IITM	19.02	73.02	14	Thane Balkun Kolshet	19.23	72.98
3	Kasar Wadavli	19.26	72.97	15	Thane Balkum Glaxo Premises	19.21	72.99
4	Belapur CBD	19.02	73.03	16	Terrace of Kopari	19.184	72.973
5	Kopripada Vashi	19.08	73.01	17	CIDCO Kharghar	19.04	73.07
6	Pimpaleshwar Mandir,Thane	19.21	72.95	18	MIDC Taloja	19.06	73.11
7	Sanpada MPCB	19.05	73.01	19	Naupada	19.19	72.97
8	Sector 2A Kalamboli	19.026	73.1	20	Nerul MPCB	19.01	73.04
9	Tondare Taloja	19.07	73.13	21	Vashi Brigade	19.07	72.99
10	Upavan Fort	19.22	72.95	22	Rabale TBIA	19.13	73
11	Airoli Fire Station	19.151	72.989	23	Nerul D Y Patil	19.046	73.024
12	Nerul STP	19.03	73.02				

The collected data from various stations, including sources, like CPCB and MPCB, was found noisy and unstructured, requiring pre-processing for analysis. The dataset includes 24 attributes for a period of 10 years, with issues, such as null values and misclassified instances. Using Google Colab and Python libraries, like Pandas, NumPy, Matplotlib, and Seaborn, the data was structured, analyzed, and visualized. Pandas handled

tabular data manipulation, NumPy supported numerical operations, and Matplotlib and Seaborn facilitated trend visualization. Python's robust ecosystem enabled efficient processing of 19,629 data points, yielding meaningful insights through graphs. The graphical representation of variation of air pollutants is shown in Figures 2 to 4.

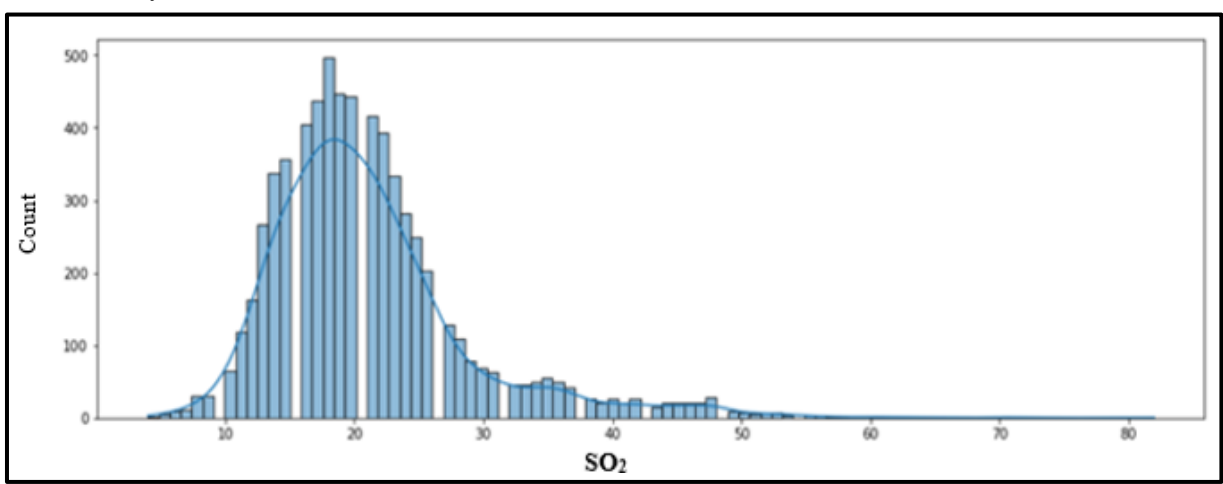


Figure 2. Variation of SO₂ with data count

The graph shown in Figure 2 illustrates the variation of SO_2 with data count as a skewed distribution. Although it seems to be a normal curve, it is sloping to

the right and is also called a positively skewed curve. The central tendency can better be assessed by median and average values.

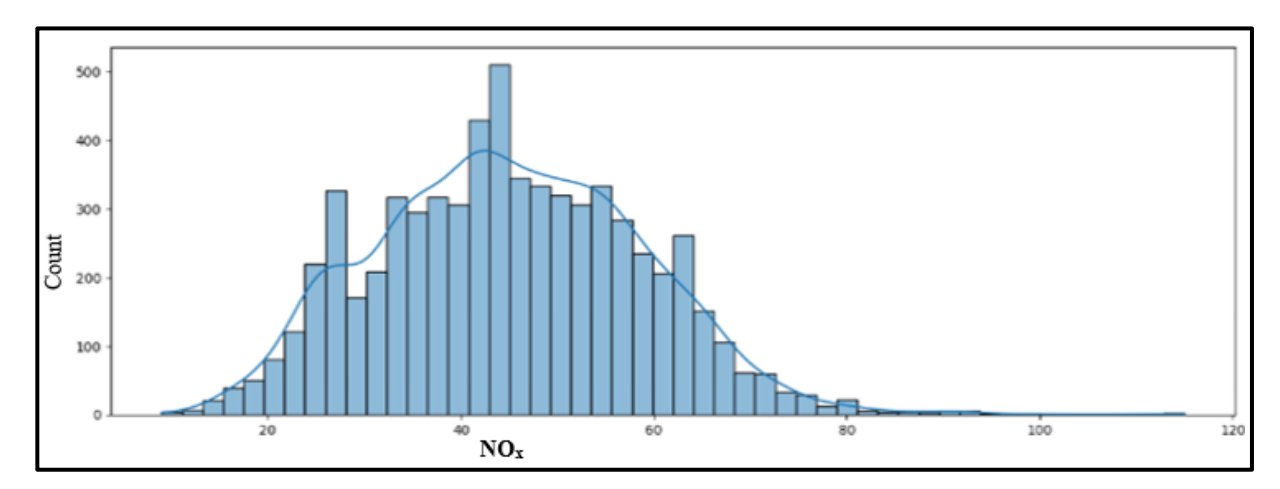


Figure 3. Variation of NO_x with data count

The graph shown in Figure 3 illustrates the variation of NO_x with data count. The frequency distribution is an almost symmetrical normal distribution and bell shaped.

The central tendency can better be assessed by median and average values.

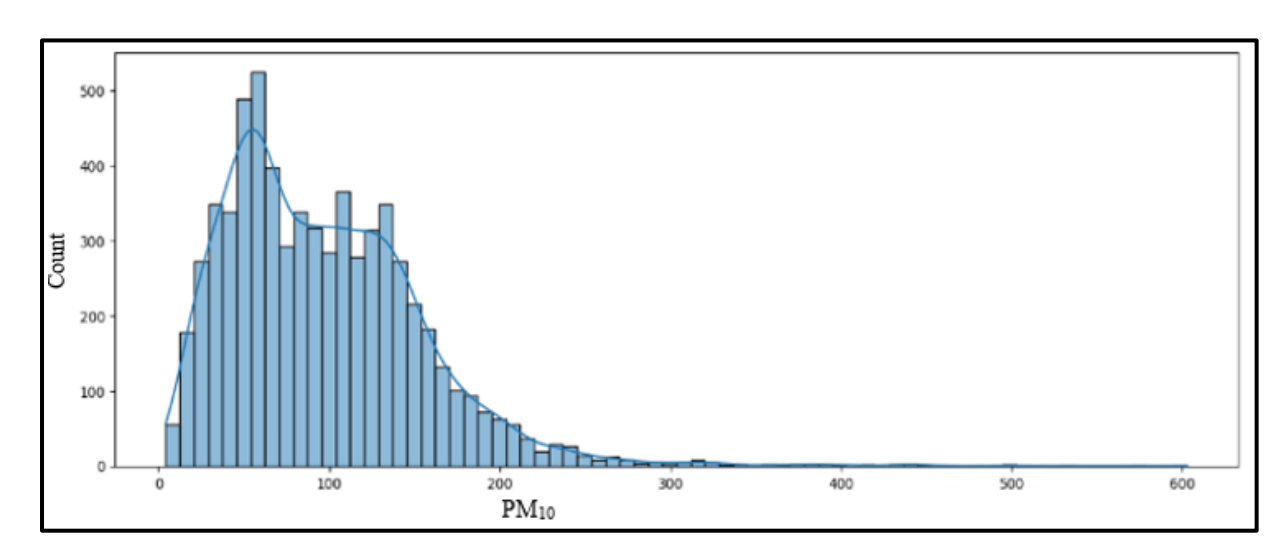


Figure 4. Variation of PM₁₀ with data count

The graph shown in Figure 4 illustrates the variation of PM_{10} with data count. This type of distribution is also a bell-shaped asymmetric curve which has a long tail at the right and hence can be termed as positively skewed. However, the curve is flattened between 100 and 200 readings on the x axis. Hence, median values can also be a better way of assessing the central tendency of data.

The scatter plots showing relationships amongst the

air pollutants under study are shown in Figure 5.

In Figure 5, it is observed that there is a strong correlation between SO_2 and NO_x . The relationship between sulphur dioxide (SO_2) and nitrogen dioxide (NO_x) in air pollution can be complex and is influenced by various factors, including emission sources, atmospheric conditions, and chemical reactions.

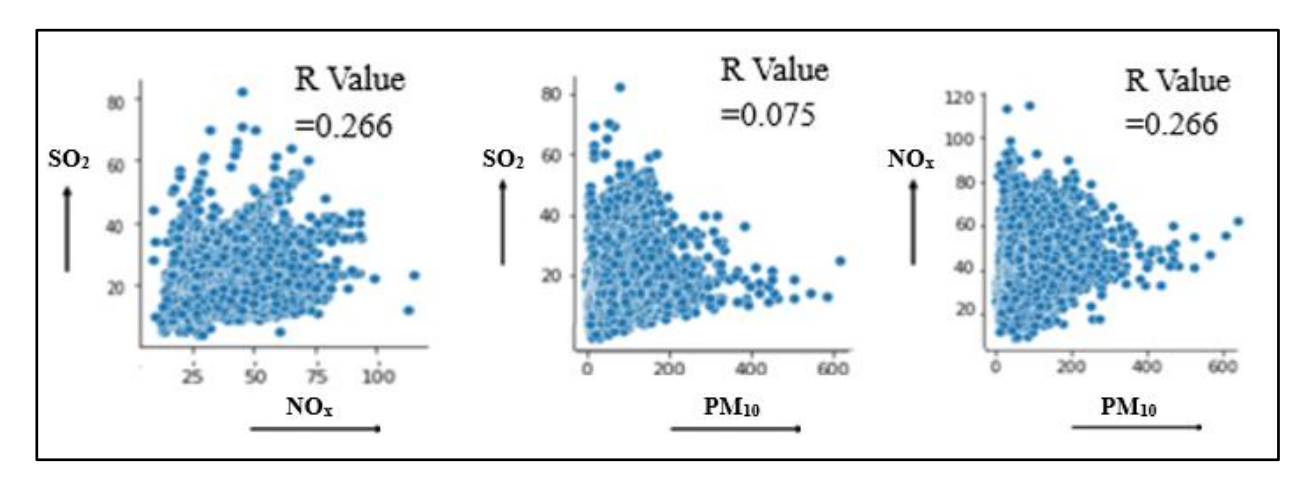


Figure 5. Scatter plot showing relationships among PM₁₀, SO₂ and NO_x

The relationship between sulphur dioxide (SO_2) and particulate matter with a diameter of 10 micrometres or less (PM_{10}) in air pollution can vary based on several factors, including emission sources, atmospheric conditions, and the characteristics of the pollutants.

The R values between PM_{10} and SO_2 (0.075) and between PM_{10} and NO_x (0.266) suggest a negligible and weak correlation, respectively. This implies that PM_{10} levels are largely independent of SO_2 and show only a weak linear association with NO_x .

Spatial Temporal Mapping

GIS 3.16 version has been used to delineate the study area consisting of 23 station points, where the air quality monitoring equipment has been placed. The daily concentrations of the criteria pollutants PM₁₀, NO_x and SO₂ have been collected from sources, like MPCB (Maharashtra Pollution Control Board), and CPCB from 23 monitoring stations.

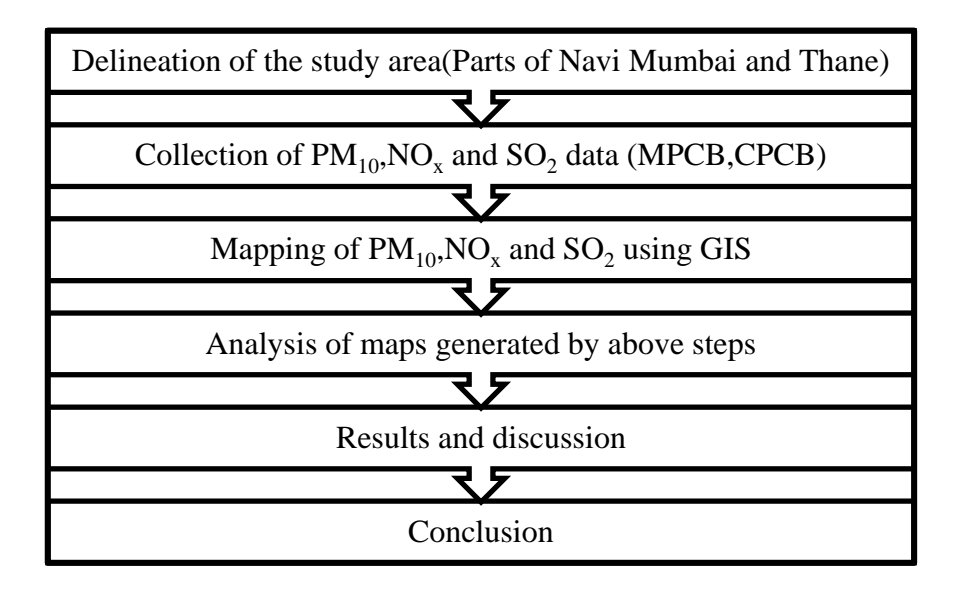


Figure 6. Methodology Flow chart

Mapping of PM₁₀, NO_x, and SO₂

The data is analysed for SO_2 , NO_x and particulate matter (PM_{10}) or Respirable Suspended Particulate Matter (RSPM). The locations under different class areas, like industrial, residential, and commercial, were monitored. Mapping of PM_{10} which is basically

Particulate Matter less than 10 micrometers, NO_x , as well as SO_2 involves some defined steps from data collection to visualization. After collection of the data, the data was processed making sure that the data points include the location (latitude and longitude), data and PM_{10} variations. The data was categorized into four

distinct seasons; namely, pre-monsoon, monsoon, post-monsoon, and winter, spanning from 2014 to 2023. Then, the data points were loaded in the GIS software making sure that the data is in a format compatible with the software (CSV format). A point layer has been created utilizing the coordinate data representing the PM_{10} monitoring stations.

Spatial Interpolation

As the main aim of this paper is the assessment of the spatial distribution of PM₁₀, NO_x, and SO₂, spatial interpolation was carried out to estimate the values of a variable at unsampled locations within an area based on the values measured at known locations. Essentially, it interpolates the missing values between observed data points to generate a seamless surface or map of the variable throughout the entire area of interest. Three methods of interpolation have been performed, IDW, Kriging and Spline and IDW gave better results as compared to the other two, as the monitoring stations across the study area are uniformly distributed. The Inverse Distance Weighted (IDW) model is commonly used and operates on the realistic assumption that a point's properties are more closely related to those of nearby locations than to those farther away (Bartier & Keller, 1996; Goutham et.al., 2018). The Inverse Distance Weighting (IDW) method provides accurate spatial interpolation results due to its assumption that nearby points have greater influence on the interpolated values than distant ones, aligning with Tobler's First Law of Geography. IDW assigns weights inversely proportional to distance, allowing for localized precision, especially in densely sampled datasets. Its deterministic nature avoids overfitting and ensures smooth surface generation, making it ideal for pollutant concentration mapping. Moreover, IDW does not require assumptions about data distribution, unlike geostatistical methods, making it suitable for heterogeneous urban environments where air quality data often exhibits non-normal spatial patterns.

The IDW method can be explained as in Equation (1) (Burrough & McDonell, 1998).

$$z(u0) = \frac{\sum_{i=1}^{n} z(ui) d_{ij}^{-p}}{\sum_{i=1}^{n} d_{ij}^{-p}}$$
 (1)

This method is widely utilized in local interpolation technique that typically utilizes a moving window to determine the area of influence. In the context of vectorbased processing, a circular moving window is frequently employed for the analysis of point data. This approach assumes that the impact of individual input points on the interpolated value at the centre of the window diminishes as the distance increases, in accordance with an inverse power relationship. More specifically, the impact is inversely related to a certain exponent (p) of the distance from the centre, as indicated in the provided formula. The estimated value at an unsampled site is denoted by z(u0), the known data points are denoted by z(ui), the distance amongst each data point and the unsampled location is denoted by dij, and p is a parameter that is usually set to 2. The weights are, in general, inversely proportional to the square of distance from unsampled site to data point. The larger the value of p, the greater the influence of nearer points. The denominator ensures that the weights sum to 1. allowing a normalized interpolation result.

RESULTS AND DISCUSSION

As discussed in the methodology section, the spatiotemporal mapping of the point pollutant concentration is carried out and the results are discussed in the current section.

Spatio-temporal Mapping of PM₁₀

Season wise maps were generated using GIS from 2014 to 2023 showing the variations of PM_{10} in the premonsoon, monsoon, post-monsoon and winter seasons, respectively. The six PM_{10} concentrations are classified as: Good, Satisfactory, Moderately polluted, Poor, Very Poor, and Severe, and each of them is depicted by a distinct colour. Health breakpoints, or favourable concentration values of air pollutants, are used to determine the likely health effects of each of these categories. The different categories are represented by 6 different colours as shown in Table 2.

Table 2. Concentrations of PM_{10} category-wise based on national guidelines (India) as per the Central Pollution Control Board (CPCB), 2023

Colour	Category	Concentration of PM ₁₀ (µg/m³)
0-50	Good	0-50
51-100	Satisfactory	51-100
101-250	Moderately poolluted	101-250
251-350	Poor	251-350
351-430	Very Poor	351-430
430+	Severe	430+

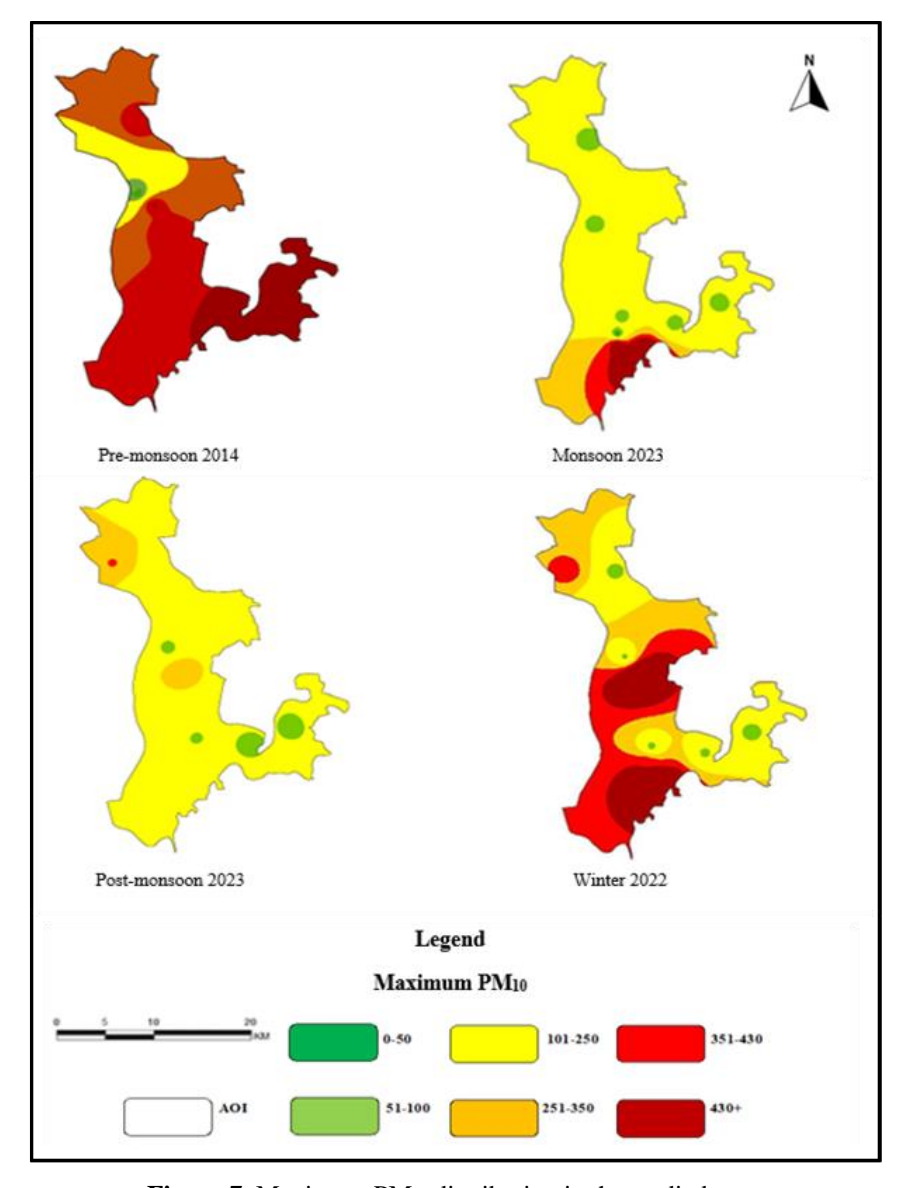


Figure 7. Maximum PM_{10} distribution in the studied zone

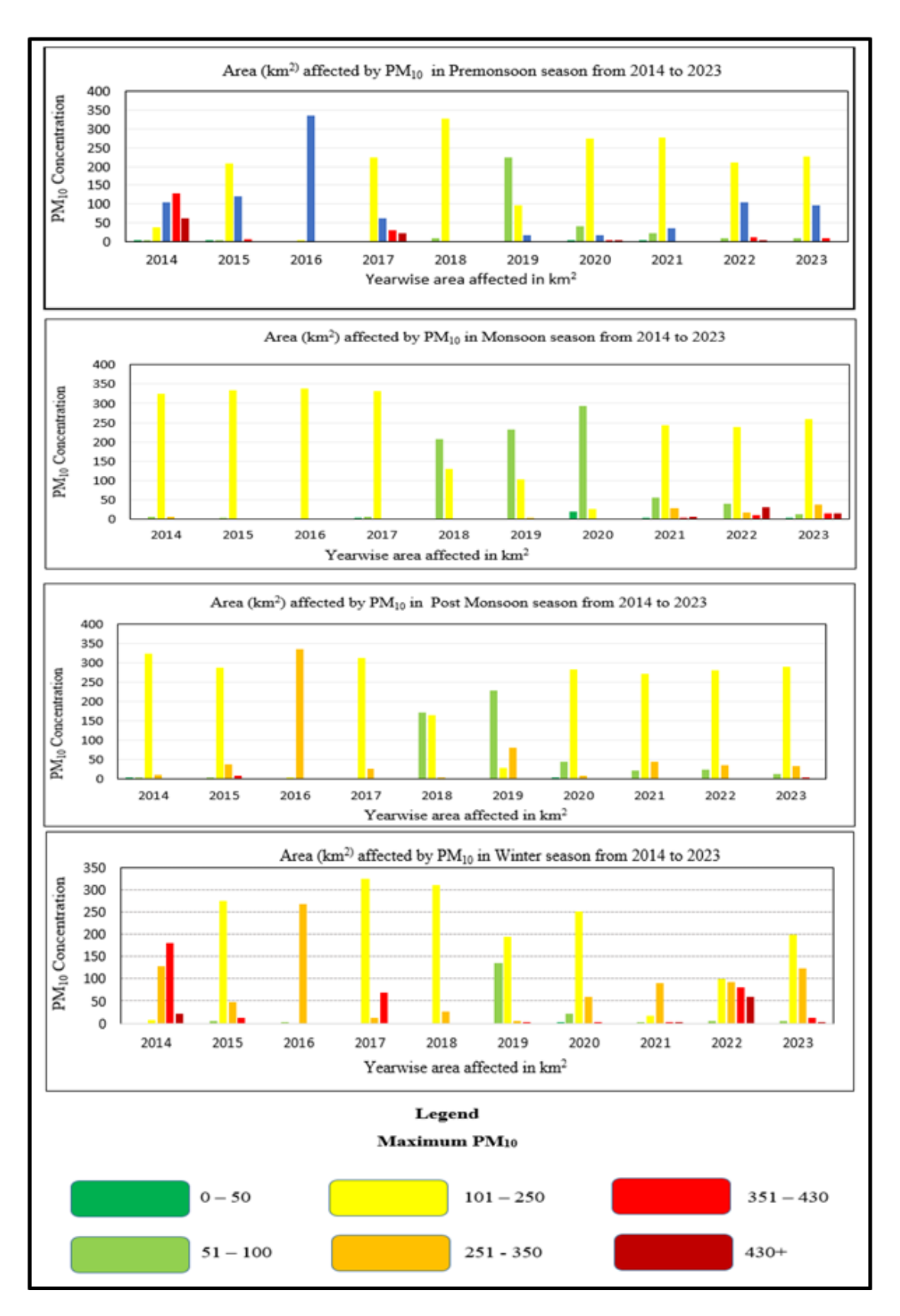


Figure 8. Categorical distribution of area affected by maximum PM₁₀

Figure 7 shows seasonal variations in maximum

 $PM_{10}\ levels$ across different periods, and Figure 8 shows

the categorical distribution of PM₁₀ affected areas. During the pre-monsoon season from 2014 to 2023, PM₁₀ concentrations in Navi Mumbai exhibited varying pollution levels. Most of the area fell within the "Moderately Polluted" category (101-250 µg/m³). The "Good" air quality category (0-50 µg/m³) covered 0.52 km² in 2014, expanded to 2.10 km² by 2020, but declined to 1.26 km² in 2021. The "Satisfactory" category (51-100 µg/m³) spanned 2.61 km² in 2014, peaked at 224.57 km² in 2019, and dropped to 7.40 km² in 2023. The "Moderately Polluted" category fluctuated, starting at 38.67 km² in 2014, peaking at 328.32 km² in 2018, and covering 226.69 km² in 2023. The "Poor" category (251-350 µg/m³) covered 104.44 km² in 2014, fluctuated over the years, and reached 95.14 km² in 2023. The "Very Poor" category (351-430 μg/m³) also showed variations, from 128.34 km² in 2014 to 8.27 km² in 2023. Meanwhile, the "Severe" category (430+ μg/m³) declined significantly from 62.74 km² in 2014 to 2.16 km² by 2022.

During the monsoon season from 2014 to 2023, PM₁₀ concentrations in Navi Mumbai were primarily in the "Moderately Polluted" category (101-250 µg/m³). The "Good" air quality category (0-50 µg/m³) spanned 0.45 km² in 2017, peaked at 18.37 km² in 2020, and decreased to 0.22 km² by 2021. The "Satisfactory" category (51-100 µg/m³) fluctuated, covering 5.90 km² in 2014, reaching a peak of 293.97 km² in 2020, and reducing to 13.34 km² in 2023. The "Moderately Polluted" category remained dominant, covering 325.77 km² in 2014 and 258.90 km² in 2023, with some variation over the years. The "Poor" category (251-350 μ g/m³) increased from 5.83 km² in 2014 to 36.65 km² in 2023. The "Very Poor" category (351-430 μg/m³) first appeared in 2021, covering 2.67 km², and expanded to 14.29 km² by 2023. Similarly, the "Severe" category (430+ µg/m³) emerged in 2021, covering 4.84 km², and grew to 14.10 km² in 2023.

During the post-monsoon season from 2014 to 2023, PM $_{10}$ concentrations in Navi Mumbai predominantly fell within the "Moderately Polluted" category (101-250 μ g/m 3). The "Good" air quality category (0-50 μ g/m 3) was minimal, covering only 0.01 km 2 in 2014 and increasing to 1.83 km 2 in 2020. The "Satisfactory" category (51-100 μ g/m 3) fluctuated, starting at 2.54 km 2 in 2014, peaking at 227.68 km 2 in 2019, and decreasing to 12.88 km 2 by 2023. The "Moderately Polluted" category consistently

dominated, ranging from 324.35 km² in 2014 to 290.42 km² in 2023. The "Poor" category (251-350 $\mu g/m^3$) showed significant variation, covering 10.60 km² in 2014, peaking at 335.82 km² in 2016, and declining to 33.67 km² in 2023. The "Very Poor" category (351-430 $\mu g/m^3$) first appeared in 2015, covering 7.70 km², and dropped to 0.52 km² in 2023. No "Severe" concentrations (430+ $\mu g/m^3$) were recorded during the period.

During the winter season from 2014 to 2023, PM₁₀ concentrations in Navi Mumbai were predominantly in the "Moderately Polluted" category (101-250 µg/m³). The "Good" air quality category (0-50 µg/m³) was scarce, covering only 0.87 km² in 2020. The "Satisfactory" category (51-100 µg/m³) fluctuated, spanning 2.54 km² in 2014, peaking at 135.48 km² in 2019, and decreasing to 4.47 km² in 2023. The "Moderately Polluted" category consistently dominated, increasing from 7.04 km² in 2014 to 198.93 km² in 2023. The "Poor" category (251-350 µg/m³) showed some variability, covering 128.97 km² in 2014 and 122.91 km² in 2023. The "Very Poor" category (351-430 µg/m³) peaked at 180.23 km² in 2014 and declined to 11.19 km² in 2023. The "Severe" category (430+ µg/m³) was recorded at 21.25 km2 in 2014 and decreased significantly to 1.71 km² in 2023.

From 2014 to 2023, PM_{10} concentrations in Navi Mumbai exhibited seasonal and spatial variations. Across all seasons, the majority of the area consistently fell within the "Moderately Polluted" category (101-250 $\mu g/m^3$), with varying extents of "Good," "Satisfactory," "Poor," "Very Poor," and "Severe" pollution levels. The "Good" and "Satisfactory" air quality categories appeared sporadically, but generally declined over time, reflecting deteriorating air quality. The "Poor" and "Very Poor" categories showed significant variability, peaking in certain years without a consistent downward trend. Although less extensive, the "Severe" category persisted, particularly during the winter and pre-monsoon seasons, highlighting periods of heightened pollution.

Spatio-temporal Mapping of NO_x

The six classes of NO_x concentration are classified as: Good, Satisfactory, Moderately polluted, Poor, Very Poor, and Severe, and each of them is depicted by a distinct colour. The different categories are represented by 6 different colours, as shown in the Table 3.

Table 3. Concentrations of NO_x category-wise based on national guidelines (India) as per the Central Pollution Control Board (CPCB), 2023

Colour	Category	Concentration of NO _x (µg/m³)
0-40	Good	0-40
41-80	Satisfactory	41-80
81-180	Moderately Polluted	81-180
181-280	Poor	181-280
281-400	Very Poor	281-400
400+	Severe	400+

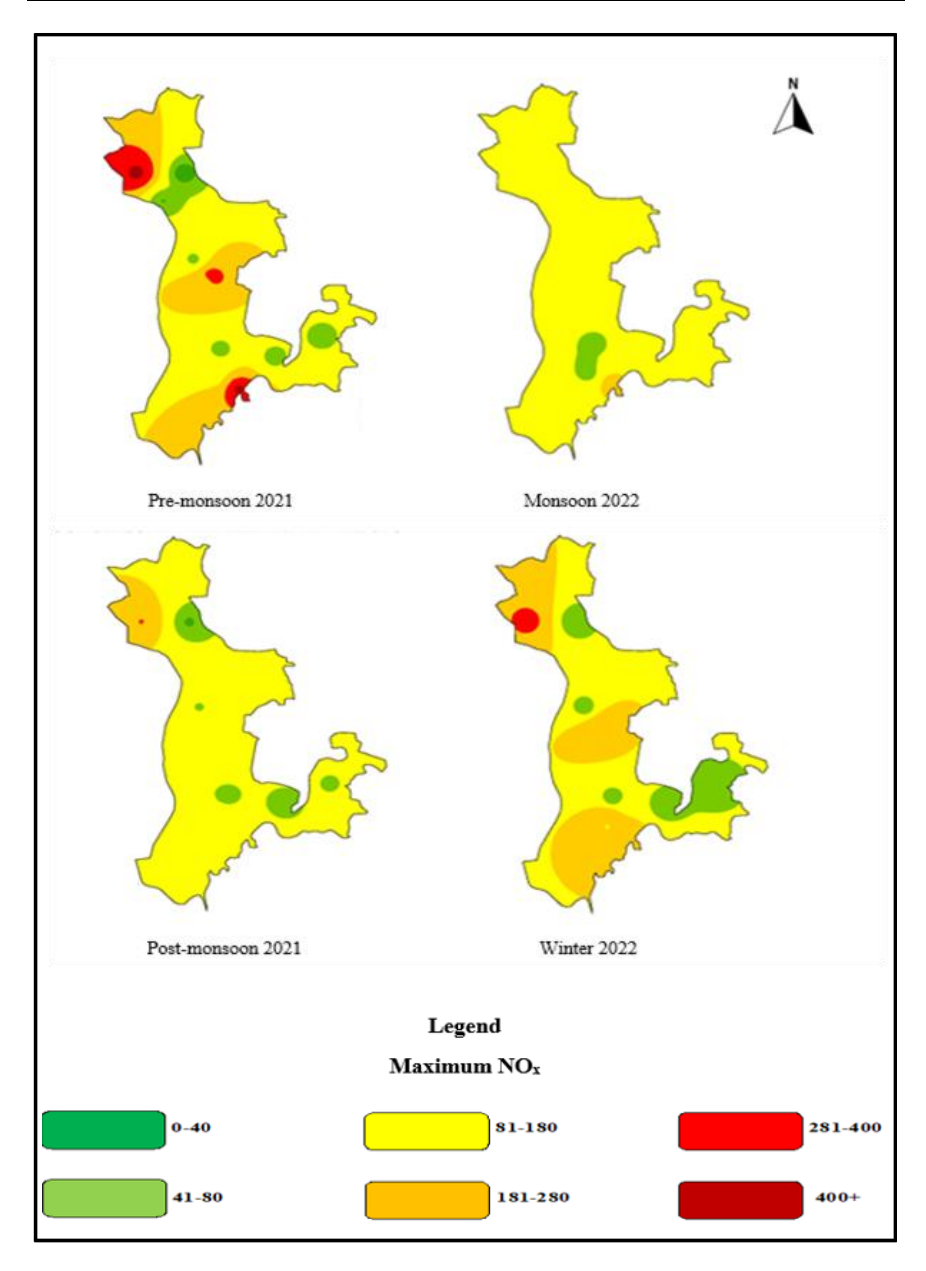


Figure 9. Maximum NO_x distribution in the studied zone

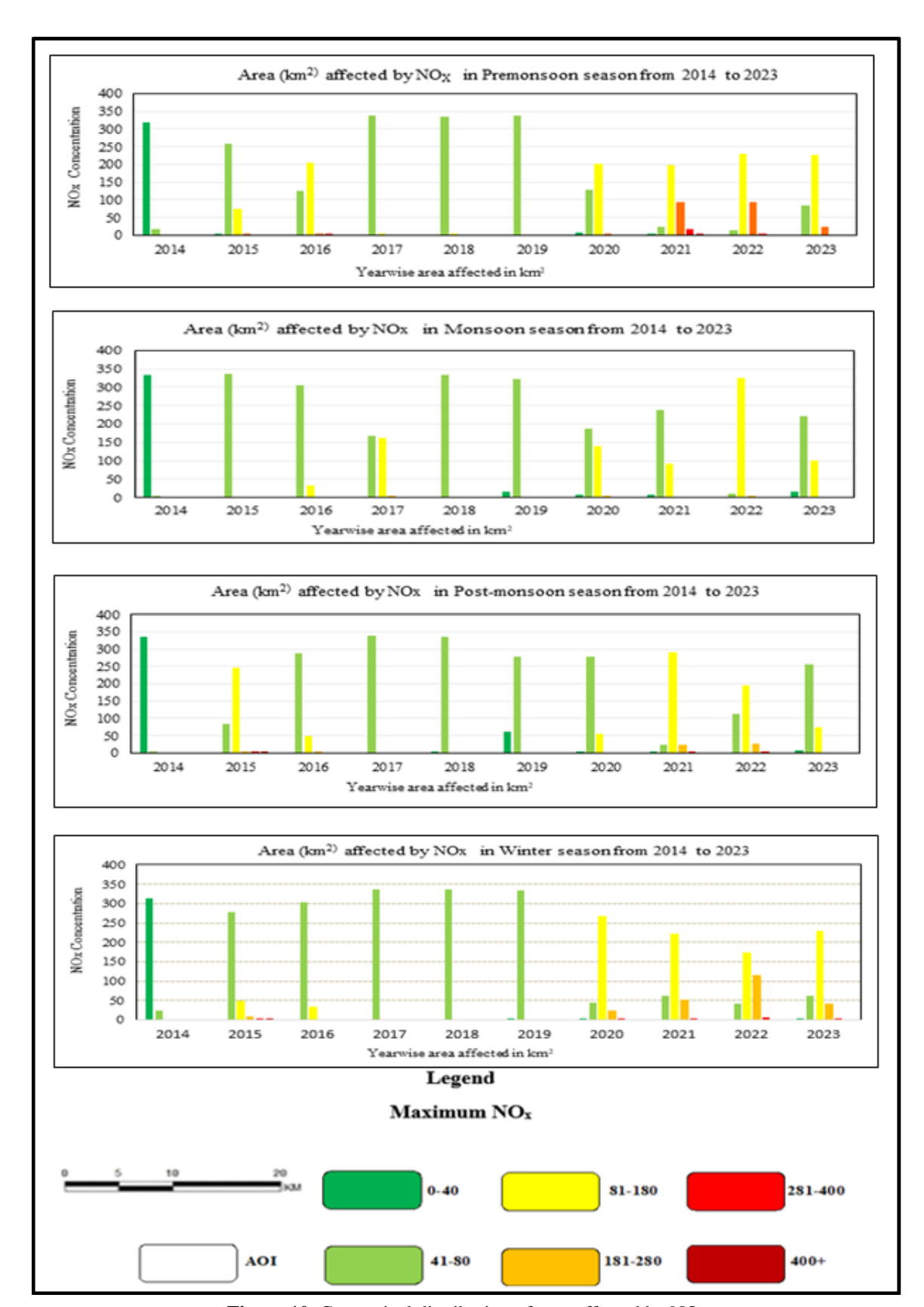


Figure 10. Categorical distribution of area affected by NO_x

Figure 9 illustrates seasonal variations in maximum

NO_x levels across different periods, while Figure 10

displays the categorical distribution of areas affected by NO_x. During the pre-monsoon season from 2017 to 2019, the majority of the area (over 300 km²) consistently fell within the 0-40 μg/m³ range of good category. This indicates better air quality during these years compared to other periods. From 2020 to 2023, there is a notable increase in the areas falling under higher NO_x concentration ranging from 81-180 µg/m³; i.e. moderately polluted category which increased significantly, peaking at 93.07 km2 in 2021 and 92.89 km2 in 2022. Areas under the 181-280 μg/m³ grew in recent years, with 25.03 km² in 2021 and 24.78 km² in 2023. Under the range 281-400 μg/m³ which is very poor category, small areas with extremely high concentrations (e.g. 3.69 km² in 2022) indicated localized pollution. During the years 2014-2016, the distribution of NO_x concentrations shows a mix of ranges, with significant areas in both 0-40 µg/m³ and 41-80 µg/m³ concentrations falling under good to satisfactory categories.

The graph illustrates the year-wise area (in square kilometers) affected by NO_x concentrations during the monsoon season from 2014 to 2023. Good category (0–40 km² range) dominates across all years, indicating that most areas experience low NO_x concentrations. Occasional spikes are visible in higher concentrations ranging from moderately polluted to poor category. In the years 2014 and 2015, a noticeable area of 333 km² contributed to good category and 337 km² area contributed to satisfactory category, respectively. In the year 2017, there was an increase in the area affected by moderately polluted category with 163 km² area observed under moderately polluted category was observed

from 2020 to 2022. The year 2023 marked the reduction in moderate and high concentrations compared to 2022, with most areas falling back into the 0-40 km² range.

In the post-monsoon season, it is observed that the good to satisfactory category dominates the study area throughout the study period of 10 years. Higher concentration ranges of moderately polluted to poor category appear periodically, with a few spikes in specific years. Substantial increase in areas with moderate to high NO_x concentrations, with 291 km² and 22.47 km², respectively, is seen in the year 2021, showing a significant growth. In 2022 and 2023, a moderate reduction in higher concentrations compared to 2021 is seen, but with residual areas still affected in yellow and orange ranges.

In the winter season, it is observed that majority of the area is dominated by satisfactory category indicated by light green colour. From 2014 to 2019, the affected areas in the good and satisfactory categories remain constantly high round about 300–340 km². Starting in 2020, there is a noticeable increase in the affected areas within the moderate concentration range. For example, 267km² in 2020,221 km² in 2021,174 km² in 2022 and 229km² in 2023. Higher concentrations of NO_x begin to emerge after 2020. 2022 and 2023; see small contributions in the highest concentration ranges.

Spatio-temporal Mapping of SO₂

The six classes of SO_2 concentration are classified as: Good, Satisfactory, moderately polluted, Poor, Very Poor, and Severe and each of them is depicted by a distinct colour. The different categories are represented by 6 different colours, as shown in the Table 4.

Table 4. Concentrations of SO₂ category-wise based on national guidelines (India) as per the Central Pollution Control Board (CPCB), 2023

Colour	Category	Concentration SO ₂ μg/m³)	
0-40	Good	0-40	
41-80	Satisfactory	41-80	
81-380	Moderately polluted	81-380	
381-800	Poor	381-800	
801-1600	Very Poor	801-1600	
1600+	Severe	1600+	

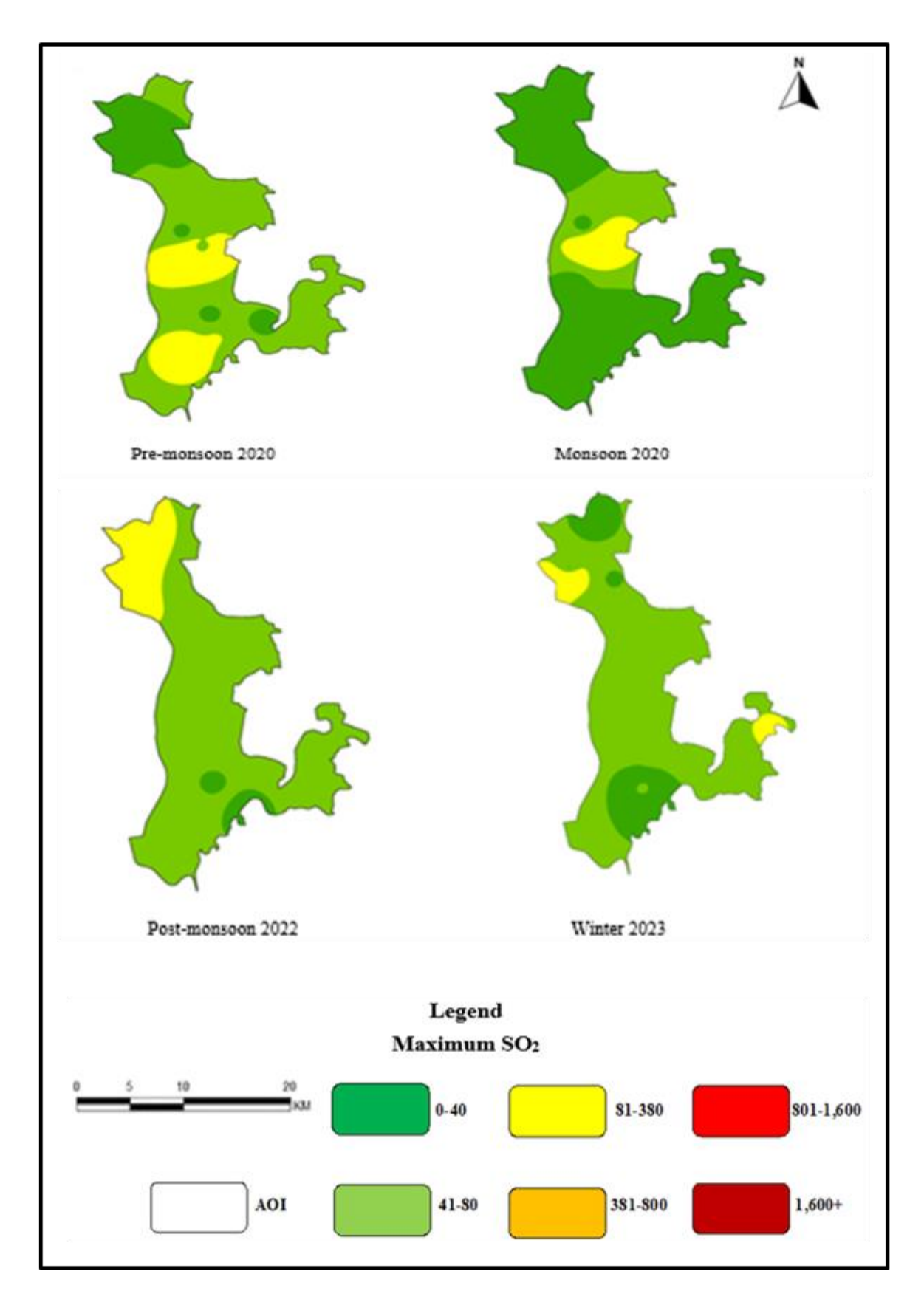


Figure 11. Maximum SO₂ distribution in the studied zone

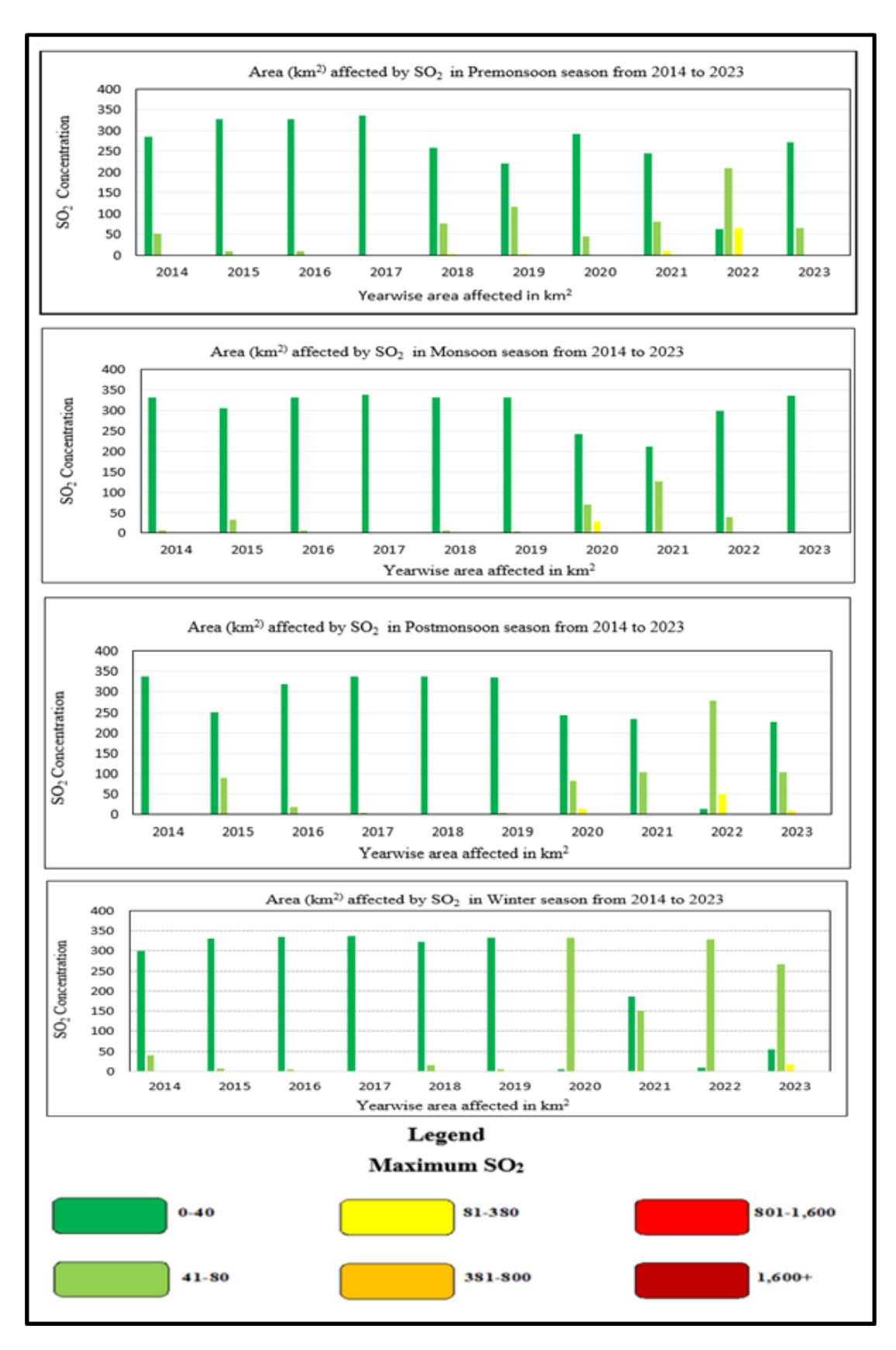


Figure 12. Categorical distribution of area affected by SO₂

Figure 11 highlights seasonal variations in maximum SO₂ levels across different periods, whereas Figure 12 shows the categorical distribution of SO₂ affected areas. The 0-40 km² concentration range of good category consistently dominates, indicating that most areas have low SO₂ concentrations across all years. From 2014 to 2017, SO₂ levels in this category remained stable with minimal variation. However, 2018 saw a noticeable drop in the 0-40 km² range, followed by a gradual recovery until 2020. Another decline occurred in 2022, with slight increases in higher concentration ranges, such as 41-80 km² and 81-380 km², reflecting higher pollution levels. By 2023, the situation improved slightly as the area affected by the 0-40 km² category increased again. The 81-380 km² category occasionally appears, but remains minor, while severe pollution ranges (poor to severe) are negligible or absent, indicating that severe SO₂ pollution is rare. Year specific anomalies include the 2018 reduction in low concentration areas, potentially linked to specific pollution events or meteorological factors, and variability in 2022 and 2023, possibly due to changes in emission sources or environmental policies.

In monsoon, the 0-40 km² concentration range (good category) overwhelmingly dominates throughout the years, indicating that most areas experience low SO₂ concentrations during the monsoon season. From 2014 to 2017, the area affected by this category remains steady, consistently exceeding 330 km² and reflecting very low SO₂ levels. A decline in the good category occurs in 2018, accompanied by slight increases in higher categories (satisfactory to moderately polluted), likely due to temporary pollution events or weather anomalies. In 2020 and 2021, the good category range experiences a significant drop, with increased areas in satisfactory to moderately polluted categories, reflecting higher pollution levels. However, the good category recovers in 2022 and 2023, with minimal areas affected by higher concentrations. Severe SO₂ concentrations representing poor category are nearly absent, indicating no extreme pollution levels. The dominance of low SO₂ levels is consistent with the cleansing effects of monsoon rains, which reduce air pollution by washing out pollutants. Year-specific variations, such as increased pollution in 2018, 2020, and 2021, are likely due to industrial or environmental factors, while 2022 and 2023 show a recovery in air quality, with the 0-40 km² category returning to near-peak levels.

In post-monsoon season, the good concentration

category in the range of 0-40 µg/m³ consistently dominates most years, indicating that the majority of the area experiences low SO₂ concentrations during this particular season. From 2014 to 2018, the area under this category remains high (above 300 km²), with minimal contributions from higher concentration categories. In 2020, the area coming under good category declines to 242.52 km², accompanied by slight increases in the satisfactory and moderately polluted categories, reflecting a temporary rise in SO₂ pollution. The satisfactory category sees a significant increase in 2022, reaching 277.51 km², indicating a notable spread of moderate SO₂ concentrations. By 2023, the good category rebounds to 226.84 km², although higher categories remain prominent. The moderately polluted category sporadically appears, particularly in 2020, 2022, and 2023, reflecting pollution spikes, while poor SO₂ concentrations (381+) remain negligible, indicating the absence of extreme pollution levels. Post-monsoon weather patterns, including reduced rainfall and stagnant atmospheric conditions, may contribute to localized pollution spikes. Year-specific observations highlight predominantly good air quality from 2014 to 2018, temporary increases in moderate pollution in 2020, a significant spread of moderate concentrations in 2022, and some recovery in 2023, with higher categories being still notable. temporary increases in moderate pollution in 2020, a significant spread of moderate concentrations in 2022, and some recovery in 2023.

The majority of the area across all years lies in the lowest concentration range, indicating good category, represented by green bars, indicating low SO₂ pollution However, occasional peaks in higher concentration ranges are observed, such as in 2021, where substantial areas fall within the good and satisfactory ranges, compared to other years. Some years, like 2022 and 2023, also show slight increases in areas affected by the satisfactory category range. Overall, the total area affected by SO₂ remains relatively stable, with minor fluctuations. The trend shows occasional spikes in moderately polluted category, but no consistent increasing or decreasing pattern over the years. This suggests that while SO₂ pollution is largely under control, specific years, such as 2021 and 2023, might have experienced isolated events leading to increased concentrations.

CONCLUSIONS

This study presents a comprehensive spatiotemporal evaluation of PM₁₀ levels across Navi Mumbai and Thane from 2014 to 2023, underscoring pronounced seasonal fluctuations and long-term shifts in air quality. In 2014, the pre-monsoon period saw 87% of the region suffering from poor to severe air quality, escalating to 98% during winter. Although municipal interventions brought some improvements by 2017, about 34% of the region continued to face unhealthy air conditions. A remarkable improvement in air quality was recorded during the COVID-19 lockdowns (2019-2020), when reduced human activity led to 66% and 12% of the total region of the study area registering satisfactory air quality. Nevertheless, this progress was short-lived. Pollution levels spiked in 2018, 2020, and 2021, largely due to rapid urban development, growing vehicular usage, ongoing construction, and the absence of rigorous enforcement of environmental regulations. The resumption of industrial activity post-lockdown, paired with increased private transport reliance, further exacerbated pollution levels. Compounding the issue occurred by meteorological conditions, like low wind speeds and temperature inversions, which hindered pollutant dispersion. By winter 2022, 68.5% of the study area showed poor to severe air quality, though this figure improved to 40% in 2023, indicating a slow, but positive, trend. Meanwhile, NO_x levels remained within safe limits until 2019, but showed a notable rise afterward, especially around industrial areas. SO₂ levels generally remained low, with sporadic increases post-2020 in selected zones.

The study highlights the value of continuous air quality monitoring through real-time sensors, integration of satellite imagery, and machine learning-based forecasting for better prediction and management. Moving forward, policy frameworks must emphasize tighter emission norms, seasonal regulations, and

REFERENCES

Abusalem, Z., Odeh, I., Al-Haqzim, N., Bazlamit, S. M., & Al-Saket, A. (2019). Analysis of air pollutants' concentration in terms of traffic conditions and road gradient in an urban area. *Jordan Journal of Civil*

sustainable practices in transport and construction. Real-world applications include creating green buffers in pollution-prone areas, promoting electric mobility, enforcing dust control at construction sites, and encouraging public participation through awareness campaigns and citizen monitoring initiatives. A coordinated, multi-dimensional approach that blends technology, policy, and community engagement is essential to achieve lasting improvements in regional air quality.

- Spatio-temporal PM₁₀ Trends: Notable seasonal and spatial variations were observed from 2014 to 2023, with 87% of the area affected in pre-monsoon 2014, increasing to 98% in winter.
- Seasonal Influences: Winter and pre-monsoon periods showed heightened pollution due to poor dispersion conditions, while monsoon failed to consistently lower pollutant levels.
- Impact of Interventions: Municipal actions led to modest improvement by 2017; COVID-19 lockdowns (2019–2020) temporarily improved air quality.
- Post-lockdown Surge: Urbanization, traffic growth, construction, and weak enforcement caused a spike in pollution in 2018, 2020, and 2021; by 2022, 68.5% of the area had poor to severe air quality.
- GIS-based Insights: Spatial interpolation using IDW method helped identify pollution hotspots and assess intervention effectiveness.
- Policy Recommendations: Enforce stricter emission norms, implement seasonal regulations, and promote green infrastructure, EV use, and better construction practices.
- Technological Enhancements: Utilize real-time sensors, satellite data, and AI-driven forecasting for better air quality management.
- Public Engagement: Citizen involvement through awareness and participatory monitoring is crucial.

Engineering, 13(3).

Alvarez-Mendoza, C.I., Teodoro, A.C., Torres, N., & Vivanco, V. (2019). Assessment of remote sensing data to model PM10 estimation in cities with a low number of air quality stations: A case study in Quito, Ecuador. *Environmental Sciences Proceedings*, 6(7), 85.

- Bartier, P.M., & Keller, C.P. (1996). Multivariate interpolation to incorporate thematic surface data using inverse distance weighting (IDW). *Computers & Geosciences*, 22, 795-799.
- Batterman, S., Jia, C., & Hatzivasilis, G. (2007). Migration of volatile organic compounds from attached garages to residences: A major exposure source. *Environmental Research*, 104, 224-240.
- Bosco, M.L., Varrica, D., & Dongarrà, G. (2005). Case study: Inorganic pollutants associated with particulate matter from an area near a petrochemical plant. *Environmental Research*, 99, 18-30.
- Burrough, P.A., & McDonnell, R.A. (1998). Principles of geographical information systems. Oxford University Press.
- Central Pollution Control Board. (2023). *National air quality index*. https://cpcb.nic.in/National-Air-Quality-Index/
- Chattopadhyay, S., Gupta, S., & Saha, R. N. (2010). Spatial and temporal variation of urban air quality: A GIS approach. *Journal of Environmental Protection*, 1(3), 264-277.
- Chhabra, S. K., Chhabra, P., Rajpal, S., & Gupta, R. K. (2010). Ambient air pollution and chronic respiratory morbidity in Delhi. *Archives of Environmental Health*, 56(1), 58-64.
- Emami, F., Masiol, M., & Hopke, P.K. (2018). Air pollution at Rochester, NY: Long-term trends and multivariate analysis of upwind SO₂ source impacts. *Science of the Total Environment*, 612, 1506-1515.
- Evagelopoulos, V., Charisiou, N.D., Logothetis, M., Evagelopoulos, G., & Logothetis, C. (2022). Cloud-based decision support system for air quality management. *Climate*, *10*(3), 39.
- Fu, X., Wang, X., Hu, Q., Li, G., Ding, X., Zhang, Y., He, Q., Liu, T., Zhang, Z., Yu, Q., Shen, R., & Bi, X. (2015). Changes in visibility with PM2.5 composition and relative humidity at a background site in the Pearl River Delta region. *Journal of Environmental Sciences*, 40, 10-19.
- Gordon, T., Balakrishnan, K., Dey, S., Rajagopalan, S., Thornburg, J., Thurston, G., Agrawal, A., Collman, G., Guleria, R., Limaye, S., Salvi, S., Kilaru, V., & Nadadur, S. (2018). Air pollution health research priorities for India: Perspectives of the Indo-U.S. communities of researchers. *Environment International*, 119, 100-108.
- Goutham, P.M., Jayalakshmi, S., & Samundeeswari, R.

- (2018). A study on comparison of interpolation techniques for air pollution modelling. *Indian Journal of Scientific Research*, 17(2), 58-63.
- Gupta, I., & Kumar, R. (2006). Trends of particulate matter in four cities in India. *Atmospheric Environment*, 40, 2552-2566.
- Huff, G., & Angeles, L. (2011). Globalization, industrialization and urbanization in pre-World War II Southeast Asia. *Explorations in Economic History*, 48(1), 20-36.
- Kampa, M., & Castanas, E. (2008). Human health effects of air pollution. *Environmental Pollution*, 151(2), 362-367.
- Kristiansson, M., Sörman, K., Tekwe, C., & Calderón Garcidueñas, L. (2015). Urban air pollution, poverty, violence and health—Neurological and immunological aspects as mediating factors. *Environmental Research*, 140, 511-513.
- Kuldeep, Sisodiya, S., Mathur, A.K., & Verma, P. (2022).
 Assessment of urban air quality for Jodhpur city by the air quality index (AQI) and exceedance factor (EF), In Advances in Materials, Manufacturing and Energy Engineering (Vol. 1, pp. 585-596). Springer Singapore.
- Kushe, V.P., Mishra, S.S., & Charhate, S. (2024).
 Analyzing coastal groundwater variability in Sindhudurg, Maharashtra: A spatio-temporal GIS approach. *Jordan Journal of Civil Engineering*, 18(4).
- Mage, D., Ozolins, G., Peterson, P., Webster, A., Orthofer, R., Vandeweerd, V., & Gwynne, M. (1996). Urban air pollution in megacities of the world. *Atmospheric Environment*, 30(5), 681-686.
- Marc, M., Bielawska, M., Simeonov, V., Namieśnik, J., & Zabiegała, B. (2016). The effect of anthropogenic activity on BTEX, NOx, SO₂, and CO concentrations in urban air of the spa city of Sopot and medium-industrialized city of Tczew located in North Poland. Environmental Research, 147, 513-524.
- National Environmental Engineering Research Institute. (2004-2013). *Ambient air quality status for six cities of India*. National Environmental Engineering Research Institute.
- Othman, N., Mat Jafri, M.Z., & San, L.H. (2010). Estimating particulate matter concentration over arid region using satellite remote sensing: A case study in Makkah, Saudi Arabia. *Modern Applied Science*, 4(11), 131-142.
- Patel, R.B., & Burkle, F.M. (2012). Rapid urbanization and the growing threat of violence and conflict: A 21st

- century crisis. *Prehospital and Disaster Medicine*, 27(2), 194-197.
- Pathakoti, M., Muppalla, A., Hazra, S., Venkata, M.D.,
 Lakshmi, K.A., Sagar, V.K., Shekhar, R., Jella, S.,
 Rama, S.S., & Vijaysundaram, V. (2021).
 Measurement report: An assessment of the impact of a nationwide lockdown on air pollution A remote sensing perspective over India. *Atmospheric Chemistry and Physics*, 21(11), 9047-9064.
- Question of Cities. (2024, August 22). Mainstreaming climate change in Navi Mumbai's development plan. https://questionofcities.org/mainstreaming-climate-change-in-navi-mumbais-development-plan/
- Sokhi, R.S., Moussiopoulos, N., Baklanov, A., Bartzis, J., Coll, I., Finardi, S., Friedrich, R., Geels, C., Grönholm, T., Halenka, T., Ketzel, M., Maragkidou, A., Matthias, V., Moldanova, J., Ntziachristos, L., Schäfer, K., Suppan, P., Tsegas, G., Carmichael, G., Franco, V., Hanna, S., Jalkanen, J.-P., Velders, G.J.M., & Kukkonen, J. (2022). Advances in air quality research-current and emerging challenges. *Atmospheric Chemistry and Physics*, 22, 4615-4703.

- Srivastava, A., & Kumar, R. (2002). Economic valuation of health impacts of air pollution in Mumbai. *Environmental Monitoring and Assessment, 75*, 135-143.
- Suman. (2021). Air quality indices: A review of methods to interpret air quality status. *Materials Today: Proceedings*, *34*, 863-868.
- Wu, J., Wilhelm, M., Chung, J., & Ritz, B. (2011). Comparing exposure assessment methods for trafficrelated air pollution in an adverse pregnancy outcome study. *Environmental Research*, 111, 685-692.
- Yang, R., Hao, X., Zhao, L., Yin, L., Liu, L., Li, X., & Liu, Q. (2022). Design and implementation of a highly accurate spatiotemporal monitoring and early warning platform for air pollutants based on IPv6. Scientific Reports, 12, Article 11825.
- Zhou, N., Cui, Z., Yang, S., Han, X., Chen, G., Zhou, Z., Zhai, C., Ma, M., Li, L., Cai, M., Li, Y., Ao, L., Shu, W., Liu, J., & Cao, J. (2014). Air pollution and decreased semen quality: A comparative study of Chongqing urban and rural areas. *Environmental Pollution*, 187, 145-152.